Comparison of the Composition and Temperature Dependences of Segmental and Terminal Dynamics in Polybutadiene/Poly(vinyl ethylene) Blends

Yiyong He, T. R. Lutz, and M. D. Ediger*

Department of Chemistry, University of Wisconsin—Madison, Madison, Wisconsin 53706

Received July 30, 2004; Revised Manuscript Received September 28, 2004

ABSTRACT: ^{13}C NMR relaxation measurements were performed on two series of miscible polymer blends: entangled polybutadiene (PB) in perdeuterated oligomeric poly(vinyl ethylene) and entangled poly(vinyl ethylene) (PVE) in perdeuterated oligomeric polybutadiene. A wide range of temperatures ($\sim T_g + 50$ K to $T_g + 200$ K) and several compositions (weight fractions of 0, 0.25, 0.5, 0.75, 1) were investigated. The segmental correlation times for the entangled components in both series of blends were extracted and compared to the corresponding terminal dynamics reported by Yang et al. The terminal dynamics have a stronger composition dependence than the segmental dynamics in PB/PVE blends. In contrast, a previous study of polyisoprene/poly(vinyl ethylene) blends revealed that the segmental and terminal dynamics exhibit equivalent dependences on the temperature and composition in that system. The Lodge/McLeish model satisfactorily fits the segmental correlation times in PB/PVE blends, but with the fit parameter ϕ_{self} different than the model prediction. We also found that the segmental dynamics of cis and trans units in the polybutadiene homopolymer have slightly different temperature dependences.

I. Introduction

The dynamic properties of miscible polymer mixtures have been investigated extensively in the past decade.[1−22] These works have established the remarkable result that, in most systems, the components exhibit distinct dynamics at both the segmental and terminal levels, even though they are molecularly well-mixed. For example, the segmental relaxation times of the two components at T_g can vary by many orders of magnitude.[1,2,12] Similar variations are observed for the monomer friction coefficients which characterize terminal relaxation.[4,10,14,16] Furthermore, in a given miscible blend, the dynamics of the different components can have significantly different temperature dependences. A clear understanding of this complexity will provide both scientific and practical opportunities.

An important long-term goal is to predict the macroscopic properties of polymer mixtures, such as the viscoelastic and transport properties, directly from the homopolymer information.[20,22,23] We imagine that this is best approached as a two-step process. First, the component segmental dynamics as a function of composition and temperature need to be accurately predicted. Then, with knowledge of the component segmental dynamics, it should be possible to predict the longer length scale dynamics which are most relevant to the macroscopic dynamic properties. Significant progress has been made toward understanding the segmental dynamics of each component in miscible polymer mixtures.[23−25] The Lodge/McLeish model[26] is the most successful model so far. Its predictions of distinct component dynamics in miscible polymer mixtures are in reasonable agreement with experiments for some but not all systems investigated.

In this paper, we address the relationship between the segmental and terminal dynamics of a given component in miscible blends. In homopolymers, it is well established that in most systems the segmental and terminal dynamics have the same temperature dependence far above the glass transition temperature (T_g).[27−29] This is consistent with the view that the segmental motions are the fundamental kinetic process which drive all other processes on longer length and time scales. In miscible mixtures, it is often assumed[22] that this same relationship between the segmental and terminal dynamics holds for each component in the mixture.

The assumption that the terminal dynamics of a given component in a miscible blend has the same temperature dependence as the segmental dynamics of that component has only been carefully tested for one system, polyisoprene/poly(vinyl ethylene) (PI/PVE) blends.[1,23] In PI/PVE, the segmental and terminal dynamics have been separately measured for both components. A variety of experimental techniques were utilized to characterize the component segmental and terminal dynamics over a wide temperature and composition range.[1−6] For each component, the segmental and terminal dynamics exhibit equivalent dependences on temperature and composition.[23] In other words, the relationship between segmental and terminal dynamics in this miscible blend is exactly the same as the relationship found for the corresponding homopolymers.

Here we test the relationship between segmental and terminal dynamics in a second miscible blend system, polybutadiene/poly(vinyl ethylene) (PB/PVE). The component terminal dynamics in PB/PVE have been thoroughly studied through a solution rheology approach by Yang et al.[16] They separately analyzed oscillatory shear measurements of "object" solutions of entangled PB in oligomeric PVE and "mirror" solutions of entangled PVE in oligomeric PB and extracted the monomeric friction coefficients, $\zeta_{PB}(\phi,T)$ and $\zeta_{PVE}(\phi,T)$. With these measurements of terminal dynamics in hand, we report here the corresponding segmental dynamics measured by NMR and explore the correlation between the segmental and terminal dynamics. PB/PVE is approximately an athermal miscible blend,[30] similar to PI/PVE in this respect.

* Corresponding author. E-mail: ediger@chem.wisc.edu.

10.1021/ma048419n CCC: $27.50
Published on Web 12/04/2004

Table 1. Characterization of PB and PVE Homopolymers

samples	M_n (kg/mol)	M_w/M_n	T_g (K)	microstructure (%) *cis*-1,4	*trans*-1,4	3,4
PB	133	1.12	178	40	50	10
dPVE	1.1	1.09	234			>82
dPB	1.3	1.12	169	36	46	18
PVE	104	1.08	261			89

In this work, ^{13}C NMR relaxation measurements were performed on two series of miscible polymer blends: entangled PB in perdeuterated oligomeric PVE and entangled PVE in perdeuterated oligomeric PB. The molecular weights of our samples match those used by Yang et al.[16] For each series of blends, we measured the spin−lattice relaxation time (T_1) and the nuclear Overhauser effect (NOE) for the entangled component. The segmental correlation times $\tau_{seg,c}$ were then extracted by fitting the NMR data to the modified Kohlrausch−Williams−Watts (mKWW) autocorrelation function and the Vogel−Tammann−Fulcher (VTF) temperature dependence and then compared to the terminal dynamics. For each component, we find that the terminal dynamics exhibit stronger composition dependence than the segmental dynamics in PB/PVE blends. The Lodge/McLeish model well fits the segmental correlation times for each component, but the fit parameter ϕ_{self} is different than the model prediction.

II. Experimental Section

Materials and Characterization. Characterization information for the homopolymers is listed in Table 1. The prefix "d" denotes perdeuteration. All the samples were purchased from Polymer Source, Inc., and prepared by anionic polymerization. The molecular weights and their distributions were determined by size exclusion chromatography. Differential scanning calorimetry measurements were carried out on a Netzsch 200 DSC. T_g is taken as the midpoint of the transition trace in heating process with a scan rate of 10 K/min after cooling the sample at the same rate from well above T_g. The microstructure information was obtained by NMR.

Each blend is composed of a perdeuterated oligomeric component and a protio-entangled component. In our NMR relaxation measurements we are only concerned with the ^{13}C resonance signals of the entangled component. The signals of interest slightly overlap those of the oligomeric component. Use of perdeuterated oligomers eliminates the proton NOE enhancement for ^{13}C signals from the oligomers and hence reduces interference with the signals of interest. Errors from overlap are small and are included in the cited uncertainties.

NMR Sample Preparation. Two series of samples were prepared by weight fraction: PB/dPVE 100/0, 75/25, 50/50, 25/75; dPB/PVE 75/25, 50/50, 25/75, 0/100. All samples were dissolved in cyclopentane first to make a dilute solution. The blend solution was stirred for 24 h to ensure complete mixing. After ~95% of the solvent was removed by blowing N_2 gas onto the solution surface, the solution was transferred to a NMR tube and coated onto the wall of the tube. Vacuum was then applied while holding the tube horizontally allowing the remaining solvent to be removed. After 72 h, a plunger was used to push the viscous coating down to the bottom of the NMR tube. The tube was then placed under vacuum again at an elevated temperature to remove bubbles in the sample and was finally sealed.

NMR Measurements. Two different relaxation measurements, T_1 and NOE, were conducted over a wide temperature range (roughly from T_g + 50 K to T_g + 200 K). T_1 was measured by the standard $\pi-\tau-\pi/2$ pulse sequence, waiting at least 8 times T_1 between the acquisition and the next pulse. NOE was measured as the ratio of ^{13}C signal intensity of the spectrum with continuous decoupling to that with inverse-gated decoupling, waiting at least 10 times T_1 between acquisitions. The number of scans used for signal averaging ranged from 8 to 128, depending on the sample and temperature. Average T_1 and NOE values, based on at least three runs, were used for further analysis at each temperature. Spectra were processed with line broadening equal to one-tenth of the line width of the spectra, followed by fitting the peak intensities as a function of delay time to a three-parameter exponential function. The uncertainty in T_1 is ±6% and in NOE is ±0.1. Measurements were performed on a Varian Inova-500 NMR spectrometer at 125.8 MHz and a Bruker DMX-300 NMR spectrometer at 25.1 MHz. Temperature was controlled to ±0.5 K and calibrated to within an uncertainty of ±2 K using a combination of an ethylene glycol thermometer[31] and melting point standards. Several tests[19] were performed to ensure that no detectable degradation took place during experiments.

In this work, we measured the ^{13}C resonance signals of the protonated component in each blend (PB component in PB/dPVE blends, PVE component in dPB/PVE blends). For PB, ^{13}C T_1 and NOE experiments were analyzed for the two methylene carbons. A cis and a trans isomeric resonance peaks are well resolved,[32] and their T_1 and NOE were measured separately. For PVE, the two resonance peaks corresponding to the backbone methylene and methine carbons are only resolved at some high temperatures. The average T_1 and NOE values of these two sp^3 carbons were used in our analysis.

NMR Relaxation Mechanism and Segmental Correlation Time. For sp^3 carbons, the dipolar interaction is the only significant relaxation mechanism for $^{13}C-H$ bond relaxation, and ^{13}C T_1 and NOE are given by[33−35]

$$\frac{1}{T_1} = Kn[J(\omega_H - \omega_C) + 3J(\omega_C) + 6J(\omega_H + \omega_C)] \quad (1)$$

$$\mathrm{NOE} = 1 + \frac{\gamma_H}{\gamma_C}\left[\frac{6J(\omega_H + \omega_C) - J(\omega_H - \omega_C)}{J(\omega_H - \omega_C) + 3J(\omega_C) + 6J(\omega_H + \omega_C)}\right] \quad (2)$$

In these expressions, ω_H and ω_C are the Larmor frequencies of ^1H and ^{13}C nuclei, respectively (with units of rad/s), n is the number of protons attached to the ^{13}C nuclei of interest (n = 2 for methylene carbons and 1 for methine carbons), γ_H and γ_C are the gyromagnetic ratios of ^1H and ^{13}C, and K is a constant which depends on the average C−H internuclear distance (equal to 2.29×10^9 s^{-2} here[36]). $J(\omega)$ is the spectral density function:

$$J(\omega) = {}^1/_2\int_{-\infty}^{\infty} G(t)\exp(-i\omega t)\,dt \quad (3)$$

Here $G(t)$ is the orientation autocorrelation function which describes the reorientation of the internuclear vector ($^{13}C-H$ in our experiments):

$$G(t) = \frac{3}{2}\langle\cos^2\theta(t)\rangle - \frac{1}{2} \quad (4)$$

Here $\theta(t)$ is the angle of a $^{13}C-H$ bond at time t relative to its original position. The bracket denotes the ensemble average over a collection of nuclei.

The mKWW function has been shown to give an excellent representation of the autocorrelation function in previous studies[29,37−39] and is used here:

$$G(t) = a_{lib}\exp\left(-\frac{t}{\tau_{lib}}\right) + (1 - a_{lib})\exp\left[-\left(\frac{t}{\tau_{seg}}\right)^{\beta}\right] \quad (5)$$

Here a_{lib} and τ_{lib} characterize the amplitude and relaxation time for the librational motion. Fits to the experimental data were insensitive to τ_{lib}, and this parameter was set equal to 1 ps. τ_{seg} and β describe a characteristic segmental relaxation time as well as its distribution. We assume that τ_{seg} follows a

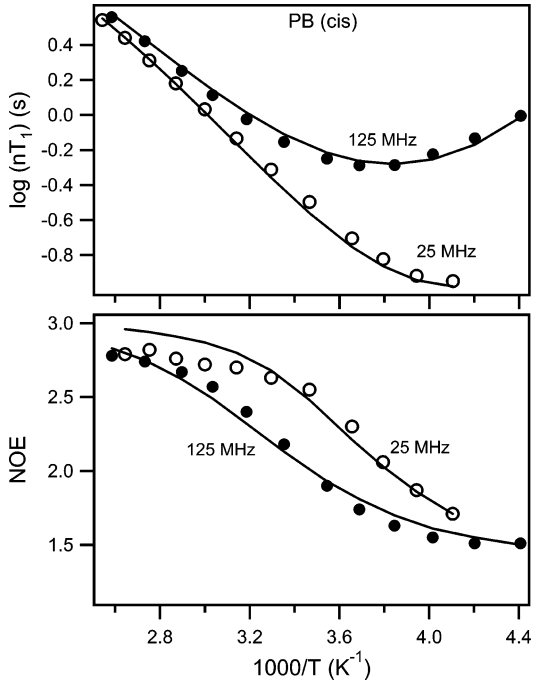

Figure 1. ^{13}C T_1 and NOE for the methylene carbons of cis units in the polybutadiene (PB) homopolymer at 125.8 and 25.1 MHz. The solid curves are fits using the mKWW autocorrelation function and VTF temperature dependence. The fit parameters are listed in Table 3.

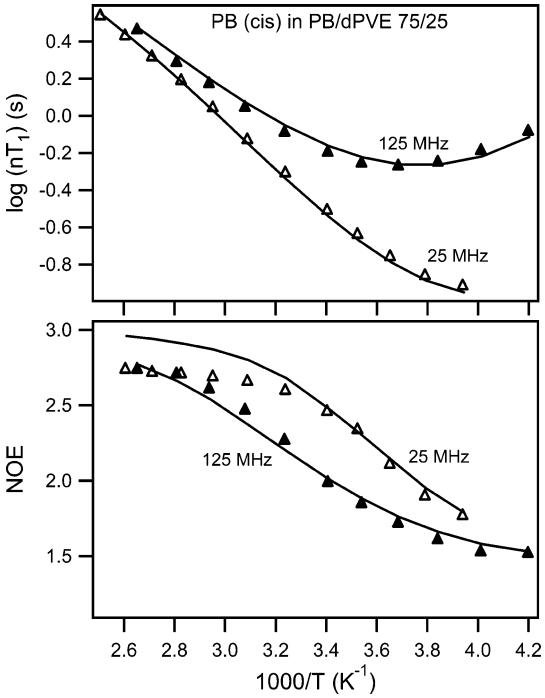

Figure 2. ^{13}C T_1 and NOE for the cis units of PB chains in PB/dPVE 75/25 blend at 125.8 and 25.1 MHz. The solid curves are fits using the mKWW autocorrelation function and VTF temperature dependence. The fit parameters are listed in Table 3.

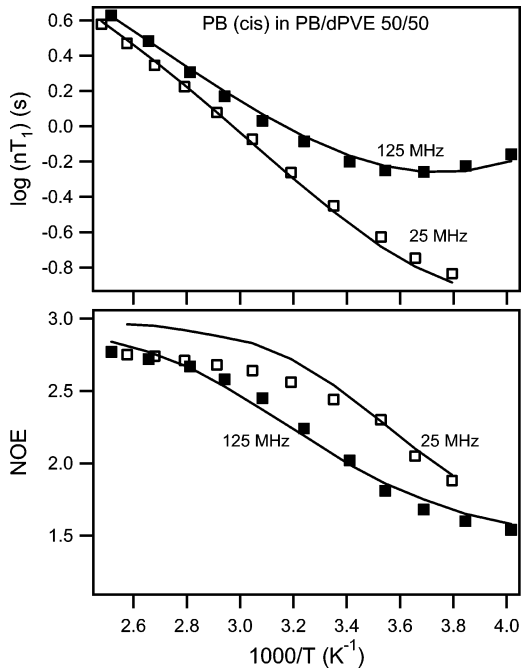

Figure 3. ^{13}C T_1 and NOE for the cis units of PB chains in PB/dPVE 50/50 blend at 125.8 and 25.1 MHz. The solid curves are fits using the mKWW autocorrelation function and VTF temperature dependence. The fit parameters are listed in Table 3.

VTF temperature dependence.[40,41] The VTF equation is equivalent to the Williams−Landel−Ferry (WLF) equation:[41]

$$\log\left(\frac{\tau_{seg}}{\tau_\infty}\right) = \frac{B}{T - T_0} \tag{6}$$

where τ_∞, B, and T_0 are constants for a given component in a particular sample. The segmental correlation time $\tau_{seg,c}$ is defined as the integral of the segmental portion of the correlation function:

$$\tau_{seg,c} = \frac{\tau_{seg}}{\beta}\Gamma\left(\frac{1}{\beta}\right) \tag{7}$$

III. Results and Discussion

A. PB Component in PB/dPVE Blends. Figures 1−4 show the T_1 and NOE data for the methylene carbons of *cis*-PB units in the homopolymer and PB/dPVE blends, measured at two magnetic fields. As summarized by the inset to Figure 4, the T_1 minimum moves to higher temperatures as the fraction of the dPVE component increases. Since the T_1 minimum approximately indicates the temperature at which the segmental dynamics occur on a 1 ns time scale, this indicates that the segmental dynamics of PB chains are slowed by the surrounding dPVE chains. Qualitatively, this is expected given the higher T_g of dPVE relative to PB. The NOE data exhibit the same variation with composition, shifting to higher temperatures with increasing dPVE fraction.

For each sample, the T_1 and NOE data for *trans*-PB units have slightly different temperature dependences than those for cis units, and their T_1 minimum positions differ by about 5 K. The data for *trans*-PB units can be found in the Supporting Information.

Superposition of the NMR Data. A model-independent way of examining the effect of mixing on segmental dynamics is to directly superpose the experimental data using temperature shifts.[42] As shown in Figure 5, nearly perfect T_1 and NOE master curves are achieved through the temperature shifts. Small vertical shifts are needed to superpose the T_1 data. The shift values used to construct Figure 5 are listed in Table 2. The excellent superposition not only shows the mixing effect on the segmental dynamics of the PB component

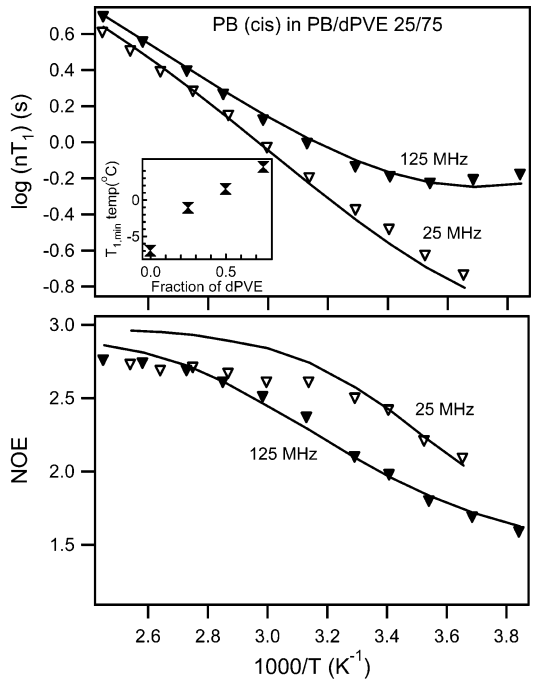

Figure 4. ^{13}C T_1 and NOE for the cis units of PB chains in PB/dPVE 25/75 blend at 125.8 and 25.1 MHz. The solid curves are fits using the mKWW autocorrelation function and VTF temperature dependence. The fit parameters are listed in Table 3. The inset shows the variation of the T_1 minimum temperature at 125.8 MHz with the dPVE fraction in PB/dPVE blends.

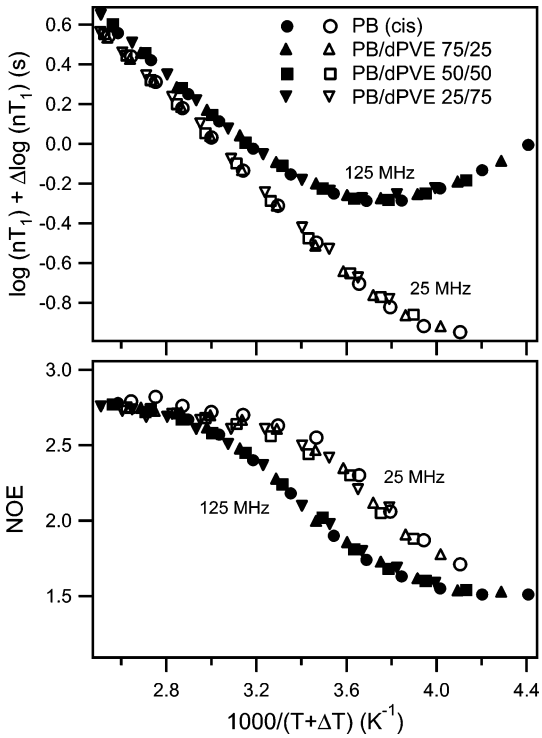

Figure 5. Superposition of T_1 and NOE data for the cis units of PB in the homopolymer and PB/dPVE blends. A single temperature shift (and vertical shift for T_1) suffice to superpose the data at 125.8 and 25.1 MHz simultaneously for a given blend.

clearly but also validates our fitting procedure and one of the assumptions of the Lodge/McLeish model (see following sections). A strong indication that these shifts are meaningful is the fact that, for a given blend, the same shifts suffice to superpose both the T_1 and NOE data at both magnetic fields.

Table 2. Horizontal and Vertical Shifts Needed To Superpose the Experimental Data of Each Component in the Blends onto the Corresponding Homopolymers

components	PB/PVE	$\Delta \log(nT_1)$ (s)	ΔT (K)	ΔT_0 (K)[a]
PB				
cis	75/25	−0.010	−5	−3
	50/50	−0.025	−7	−6
	25/75	−0.045	−10	−10
trans	75/25	−0.020	−6	−5
	50/50	−0.050	−10	−8
	25/75	−0.11	−16	−15
PVE	75/25	+0.015	+33	+37
	50/50	+0.020	+22	+26
	25/75	+0.015	+12	+14

[a] From Table 3.

The superposition of the data for trans units also works well (not shown). However, their temperature shifts ΔT are slightly different than cis units, as shown in Table 2. Such a difference is beyond experimental error (for 50/50 and 25/75 PB/PVE) and indicates that the segmental dynamics of cis and trans units in PB chains have different composition dependences upon mixing (see below).

Fits to the mKWW and VTF Functions. Although the superposition provides direct information about the mixing effect on the segmental dynamics, fitting the experimental data to a model correlation function allows us to extract the segmental relaxation times and have a more quantitative description of the experimental results. Since it was found in previous studies[37−39] that the mKWW function (eq 5) provides excellent fits to the NMR relaxation data, we employed it here in combination with the assumption of VTF temperature dependence (eq 6) for the segmental relaxation times.

For each sample, fitting was performed on both T_1 and NOE at two magnetic fields simultaneously using eqs 1−6 for either cis or trans units. The NMR experiments do not directly measure the orientation autocorrelation function $G(t)$. In our fitting, we make an initial guess about the fit parameters, calculate the resulting T_1 and NOE, and then optimize the parameters to provide the best fit to the NMR data. There are five unknown parameters in this procedure: a_{lib}, β, τ_∞, B, and T_0. Because of the relatively small range of correlation times probed by NMR experiments, B and T_0 are highly correlated with each other, and usually some constraints are desirable. First we fit the T_1 and NOE data of the PB homopolymer with no constraint. Both cis and trans units produce the same B value of 500 K. Then we fixed B to that value when fitting the NMR data of the PB component in the blends. This approximation is supported by the excellent superposition in Figure 5. The fit parameters are summarized in Table 3 and yield reasonable fits to the experimental data. The fits to the data of cis units are shown in Figures 1−4 by the solid lines. The mismatch at high NOE values is due to the absence of long time relaxation in the mKWW equation (eq 5) and does not indicate a failure to accurately describe the segmental dynamics.[38,39] The fits to the data of trans units have similar quality but are not shown here.

One indication of the robustness of our fitting procedure is that T_0 closely tracks the variation of the T_1 minimum (ΔT_0 vs ΔT in Table 2). For the PB homopolymer, the parameter β from the fit agrees with the value

Table 3. Fit Parameters for Segmental Dynamics of PB and PVE in Homopolymers and Blends

fit parameters		pure PB	PB/PVE 75/25	PB/PVE 50/50	PB/PVE 25/75	pure PVE
PB[a]						
cis	β	0.39	0.39	0.39	0.39	
	τ_∞ (ps)	0.050	0.058	0.050	0.047	
	T_0 (K)	138	141	144	148	
	a_{lib}	0.31	0.33	0.34	0.36	
trans	β	0.39	0.39	0.39	0.39	
	τ_∞ (ps)	0.102	0.116	0.113	0.104	
	T_0 (K)	130	135	138	145	
	a_{lib}	0.38	0.43	0.46	0.52	
PVE[b]	β		0.51	0.51	0.49	0.49
	τ_∞ (ps)		0.50	0.49	0.43	0.42
	T_0 (K)		181	192	204	218
	a_{lib}		0.37	0.37	0.37	0.38

[a] VTF parameter B was constrained to 500 K in all the blends. [b] VTF parameter B was constrained to 513 K in all the blends.

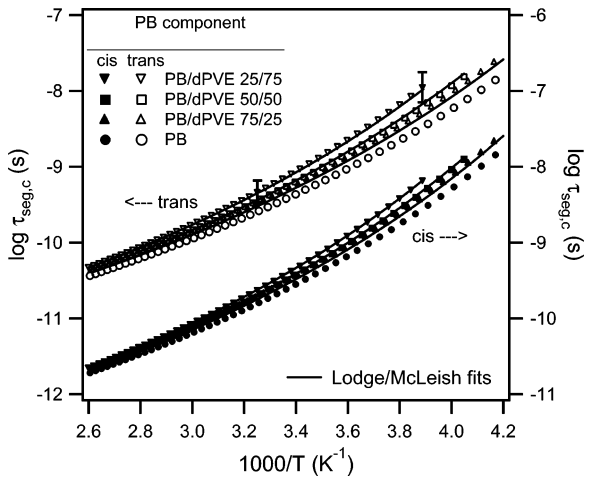

Figure 6. Segmental correlation times (calculated from the fit parameters in Table 3 and shown as symbols) for both cis and trans units of PB in the homopolymer and PB/dPVE blends. Representative error bars are shown and reflect the uncertainty associated with the fitting procedure. The solid lines are fits to the Lodge/McLeish model with ϕ_{self}(*cis*-PB) = 0.71 and ϕ_{self}(*trans*-PB) = 0.59.

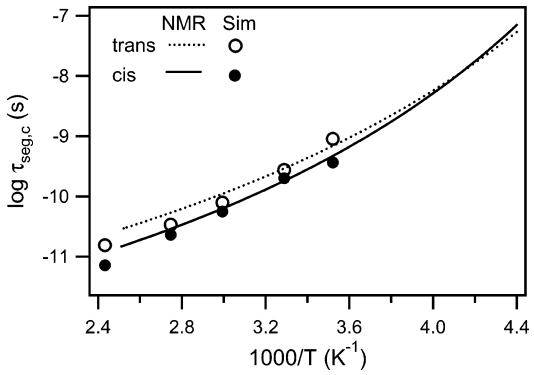

Figure 7. Segmental correlation times of the cis and trans units in the PB homopolymer from MD simulations (ref 46) and NMR experiments (Table 3). The cis and trans geometric isomers exhibit slightly different segmental dynamics in both experiments and simulations. The simulation results were shifted to higher temperature by 11 K to account for the molecular weight difference.[48]

from dielectric relaxation[43,44] within experimental error. Because of the correlations between B and T_0 and between a_{lib} and β, these parameters have substantial uncertainties: B is accurate within ±100 K, T_0 is accurate within ±15 K, and both a_{lib} and β have an uncertainty of ±0.1.

Segmental Correlation Times. The segmental correlation times $\tau_{seg,c}$ of the PB homopolymer and PB component in the blends were calculated from the fit parameters in Table 3 and are presented in Figure 6 as the symbols. As expected from the homopolymer T_gs and consistent with the superposition suggestion, $\tau_{seg,c}$ of the PB component at a given temperature increases as the dPVE fraction increases. This effect is more pronounced at low temperatures. The uncertainty in the reported $\tau_{seg,c}$, as reflected by different fitting procedures and variation of the fit parameters, is shown by the representative error bars in Figure 6. $\tau_{seg,c}$ of the PB homopolymer at the low temperature end agrees reasonably with dielectric relaxation studies in the literature.[44,45] In a given sample, the segmental dynamics of *cis*- and *trans*-PB units have slightly different temperature and composition dependences. Please note that $\tau_{seg,c}$ for cis and trans units are similar but plotted on different axes in Figure 6 for clarity.

Comparison of the Dynamics of Cis and Trans Units in PB. Figure 7 compares the segmental dynamics of cis and trans units in the PB homopolymer. The cis units have slightly stronger temperature dependence and slower dynamics than the trans units over the temperature range of study. Molecular dynamics (MD) computer simulations reproduce this small difference in segmental dynamics,[46] as shown in the figure. The difference shown here between the dynamics of cis and trans units in the PB homopolymer might explain the failure of time−temperature superposition of DR data on PB homopolymers.[47] In Figure 7, the simulation data are shifted to higher temperature by 11 K to account for the T_g dependence of molecular weight.[48]

Lodge/McLeish Model. The Lodge/McLeish model provides a framework for interpreting and predicting the component dynamics in miscible polymer mixtures.[26] It assumes that the segmental relaxation process of a given segment in a polymer mixture is affected by the local composition in a surrounding region with a length scale of the Kuhn segment l_k. The effective local concentration ϕ_{eff} is given by

$$\phi_{eff} = \phi_{self} + (1 - \phi_{self})\phi \tag{8}$$

Here ϕ_{self} is the self-concentration of the considered polymer. It is determined from the volume fraction occupied by one Kuhn length of the polymer inside a volume $V = l_k^3$:

$$\phi_{self} = \frac{C_\infty M_0}{k\rho N_{av} V} \tag{9}$$

Here M_0 is the molar mass of the repeat unit, N_{av} is

the Avogadro constant, k is the number of backbone bonds per repeat unit, ρ is the bulk density, and C_∞ is the characteristic ratio.

The model associates the average local concentration ϕ_{eff} for each component with a local glass transition temperature $T_{g,\text{eff}}(\phi) = T_g(\phi_{\text{eff}})$, which is assumed to obey the Fox equation:

$$\frac{1}{T_g(\phi_{\text{eff}})} = \frac{\phi_{\text{eff}}}{T_g^A} + \frac{1-\phi_{\text{eff}}}{T_g^B} \tag{10}$$

The component dynamics in the mixtures can be predicted by correlating the changes in $T_{g,\text{eff}}$ with the changes in T_0

$$T_{0,i}(\phi) = T_{0,i} + [T_{g,\text{eff}}^i(\phi) - T_g^i] \tag{11}$$

and by assuming that the remaining VTF parameters (B, τ_∞) do not change with mixing.[25] Here "i" denotes component A or B.

Comparison to the Lodge/McLeish Model. The Lodge/McLeish model successfully fits the segmental correlation times with $\phi_{\text{self}}(cis\text{-PB}) = 0.71 \pm 0.14$ and $\phi_{\text{self}}(trans\text{-PB}) = 0.59 \pm 0.11$. The fits are plotted in Figure 6 as the solid lines. The only input information in the fitting process is the segmental dynamics of the homopolymer; ϕ_{self} is an adjustable parameter. For each geometric isomer, the ϕ_{self} value and the $\tau_{\text{seg,c}}$ curve of the homopolymer generate the three fitting curves. The uncertainty in the reported ϕ_{self} values is estimated by the point where the deviation from the fitting is comparable to the experimental uncertainty. The fits well describe the variation in PB component dynamics with the composition and temperature.

The values of ϕ_{self} obtained from the fitting procedure (0.71 and 0.59) are quite different than the prediction of the Lodge/McLeish model ($\phi_{\text{self}} = 0.29$), calculated using eq 9. We propose three possible reasons for this disagreement: (1) Some modifications are needed to eq 9. As Lodge and McLeish pointed out, eq 9 could easily be modified by a multiplicative constant of order unity, as the choice of $V = l_k^3$ is somewhat arbitrary. For example, a spherical or cylindrical volume could be chosen instead of a cube. In addition, the assumption that the Kuhn segment is the length scale relevant for segmental relaxation may not be exactly correct. (2) The Lodge/McLeish model implicitly assumes that the dynamics of the two components are strongly coupled with each other. However, some previous studies have suggested that the segmental motions of the two components might weakly couple with each other if the two homopolymers have large structure disparity.[9,12] This may happen in the case when the high-T_g component has a large side group while the low-T_g component has no side group or a small flexible side group. The weak coupling hypothesis reasonably reconciles the unusually fast dynamics of the low-T_g component in poly(ethylene oxide)/poly(methyl methacrylate) (PEO/PMMA)[12] and poly(vinyl methyl ether)/polystyrene (PVME/PS)[8,9] blends. It is easy to imagine the local conformational relaxation of PEO in the cage formed by surrounding PMMA segments since PEO chains have no side group. In PVME/PS blends, the methoxyl side group is small and flexible. In PB/dPVE blends, the PB chain may be similar in behavior to the PEO chain as it has no side group, and there may be only weak coupling between PB and dPVE chains in these blends. This tentative explanation is somewhat similar to the idea of coupling model of Ngai and Roland.[49] (3) The Lodge/McLeish model neglects thermal concentration fluctuations while other models incorporate this effect. We expect this effect to be small compared to the self-concentration.

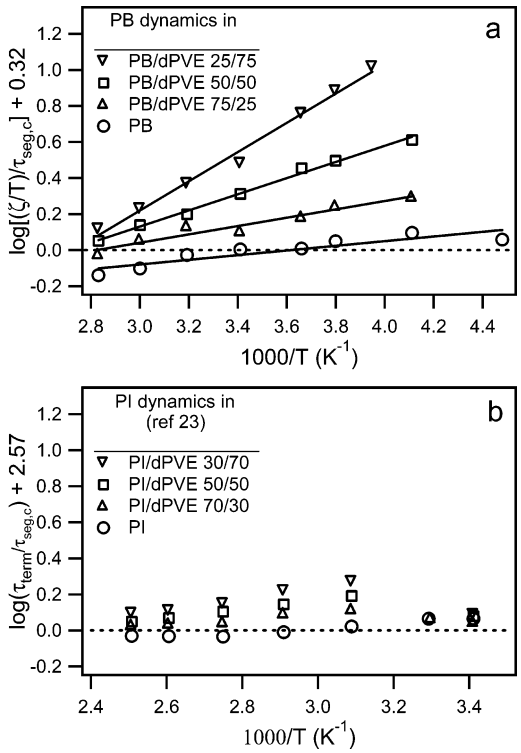

Figure 8. (a) Ratio of the terminal dynamics (ζ/T) to the segmental dynamics ($\tau_{\text{seg,c}}$) for PB in the homopolymer and PB/dPVE blends. ζ (in units of dyn·s/cm) are taken from ref 16. $\tau_{\text{seg,c}}$ (in units of seconds) are calculated from the fit parameters of *cis*-PB in Table 3. A vertical shift is applied to place the homopolymer data on the horizontal zero line, as indicated. While the terminal dynamics essentially track the temperature dependence of the segmental dynamics in PB homopolymer, the terminal dynamics exhibit a stronger composition and temperature dependence than the segmental dynamics in the blends. (b) Ratio of the terminal to segmental relaxation times for PI in the homopolymer and PI/PVE blends (data from ref 23). For both the homopolymer and blends, the terminal dynamics essentially tracks the temperature and composition dependences of the segmental dynamics within experimental error.

Comparison of the Segmental and Terminal Dynamics. In a recent study of PI/PVE blends,[23] the terminal dynamics of each component were found to have essentially the same temperature and composition dependences as the segmental dynamics; i.e., the variation of the terminal dynamics with composition and temperature completely tracks that of the segmental dynamics upon mixing. It is of great interest to see whether this simple relationship also exists in PB/PVE blends. Here we compared our segmental dynamics data to the corresponding terminal dynamics (obtained from rheological measurements) reported by Yang et al.[16]

A straightforward way to compare the composition and temperature dependences of the segmental and terminal relaxation times is to plot their ratio vs temperature (Figure 8a). The terminal relaxation time is represented by ζ/T, which reflects the changes in terminal dynamics in such a way as to account for the changes in entanglement with composition. For the PB homopolymer, this ratio is a flat line within the experimental uncertainty (±0.3 decades). This is consistent

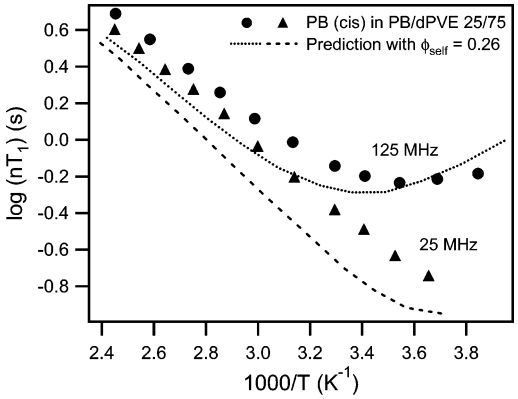

Figure 9. Lodge/McLeish model prediction of ^{13}C T_1 for the *cis*-PB in PB/dPVE 25/75 blend, assuming that the segmental dynamics follow the same composition dependence as the terminal dynamics ($\phi_{self} = 0.26$). The symbols are the same data as Figure 4. The mismatch between the points and lines indicates that the segmental dynamics (as reflected by T_1) do not have the same composition dependence of the terminal dynamics.

with the documented conclusion that the segmental and terminal dynamics of most homopolymers have the same temperature dependences far above T_g.[27−29] This simple relationship does not hold for PB in PB/PVE blends, as the ratio exhibits a substantial dependence on both composition and temperature. Thus, the terminal dynamics of the PB component in PB/PVE blends have different composition and temperature dependences than their corresponding segmental dynamics. For comparison, we present the same plot for PI in PI/PVE blends (data from ref 23) in Figure 8b. To allow a clear comparison, the data were plotted in the similar temperature window (roughly above T_g + 50 K) and with the same vertical scale. The terminal dynamics of the PI component in PI/PVE blends have essentially identical (within experimental error of ±0.3 decades) composition and temperature dependences as their corresponding segmental dynamics. Only the segmental dynamics of *cis*-PB units are compared to the terminal dynamics in Figure 8a. The analogous comparison using *trans*-PB units yields qualitatively the same conclusion.[50]

Another way to compare the composition dependences of the segmental and terminal dynamics is to use the Lodge/McLeish fit parameter ϕ_{self}. The segmental dynamics of the PB component in PB/dPVE blends have an average ϕ_{self} of 0.65 ± 0.13 (0.71 for *cis*-PB and 0.59 for *trans*-PB), while the terminal dynamics have been previously reported to have a ϕ_{self} of 0.26 ± 0.05.[25] Since a smaller ϕ_{self} implies a stronger composition dependence, this analysis is consistent with Figure 8a. Since PB is the low-T_g component in these blends, the smaller ϕ_{self} value for the terminal dynamics also indicates that the terminal relaxation in the blends has a stronger temperature dependence than the segmental relaxation; again, this is consistent with Figure 8a.

We can also see the difference in composition dependence between the segmental and terminal dynamics by making a comparison directly in terms of the NMR data. In this way we can avoid the assumptions implemented in our fitting procedure. An example of such a comparison was made on the PB/dPVE 25/75 blend and shown in Figure 9. The symbols are the experimental T_1 data from Figure 4. The dotted lines are predictions from the Lodge/McLeish model, if we assume that the segmental dynamics of PB follow the same composition dependence as its terminal dynamics ($\phi_{self} = 0.26$). Clearly this assumption is not valid as the mismatch is much larger than the experimental error (±6%).

It is not clear why the terminal dynamics exhibit stronger composition and temperature dependences than the segmental dynamics for PB blended with PVE while in PI/PVE the composition and temperature dependences of the terminal dynamics for each component essentially track its segmental dynamics.[23] The stronger composition and temperature dependences of the terminal dynamics compared to the segmental dynamics suggest that some factors strongly affecting the terminal relaxation are less significant at the segmental level. The weak coupling hypothesis discussed above is able to qualitatively reconcile the phenomena. In the framework of weak coupling, the absence of side groups allows conformational relaxation for PB segments without requiring significant rearrangements of nearby PVE segments. In contrast, terminal relaxation involves variation of end-to-end vectors and thus would require the cooperative movement of both PB and its nearby PVE segments. We speculate that strong coupling in this sense should exist in the terminal dynamics of all miscible polymer blends. An argument in favor of this explanation is that the fitted ϕ_{self} value for terminal dynamics (0.26) is quite close to the Lodge−McLeish prediction (0.29). The Lodge−McLeish paper[26] argues that their prediction for ϕ_{self} applies to the smallest Rouse segment, which would be somewhat larger than the length scale of segmental motion. Thus, our "weak coupling" explanation might apply only to the segmental dynamics in this system and not to longer length scale motions. This explanation is further strengthened by the similar results reported in PEO/PMMA blends. The terminal dynamics of PEO in a 20% PEO/PMMA blend also exhibits much stronger composition and temperature dependences than the segmental dynamics.[12]

B. PVE Component in dPB/PVE Blends. In this section we will follow the same procedure as used above to analyze the data for the PVE component in dPB/PVE blends. Figure 10 shows the average T_1 and NOE data for the two backbone carbons of PVE in the homopolymer and dPB/PVE blends. In contrast to the trend of the PB component in PB/dPVE blends, here the T_1 minimum and NOE shift to lower temperatures with mixing, indicating that the dynamics of PVE get faster upon blending. The NOE data at 25.1 MHz are not presented due to interference from dPB signals at this low magnetic field.

Superposition of the NMR Data. Nearly perfect T_1 and NOE master curves are achieved by making simultaneous temperature shifts to the T_1 and NOE data at the two magnetic fields. Small vertical shifts are also needed to superpose the T_1 data. The resulting superposition curves are shown in Figure 11, and the shift values are listed in Table 2.

Fits to the mKWW and VTF Functions. We used exactly the same strategy as in IIIA to fit the NMR data.[51] Fitting the data for the PVE homopolymer generates a B value of 513 K. We fixed B to this value when fitting the data for the PVE component in the blends. The use of this constraint is supported by the excellent superposition in Figure 11. The fit parameters are listed in Table 3, and the resulting fits are excellent (solid lines in Figure 10). As expected, ΔT_0 closely tracks

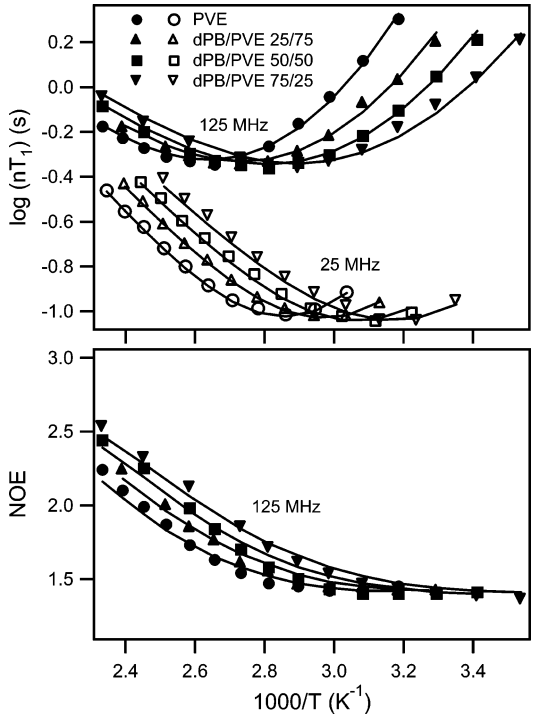

Figure 10. ^{13}C T_1 and NOE for the backbone carbons of PVE in the homopolymer and dPB/PVE blends at 125.8 and 25.1 MHz. The solid curves are fits using the mKWW autocorrelation function and VTF temperature dependence. The fit parameters are listed in Table 3.

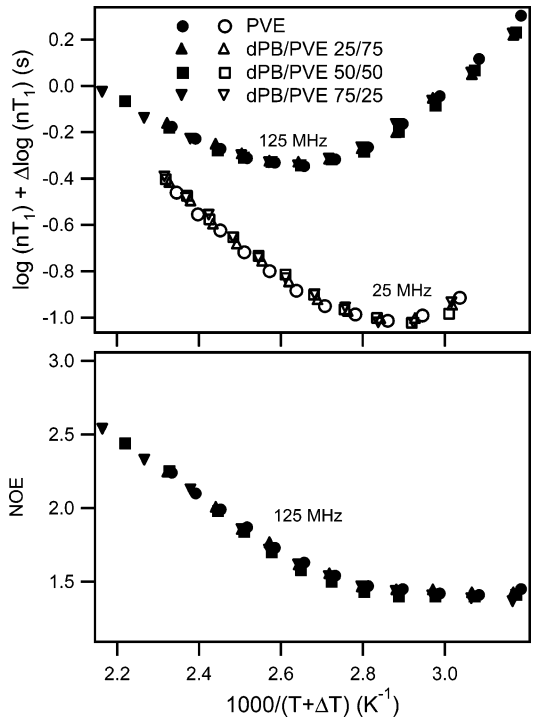

Figure 11. Superposition of T_1 and NOE data for PVE in the homopolymer and dPB/PVE blends. A single temperature shift (and vertical shift for T_1) suffice to superpose the data at 125.8 and 25.1 MHz simultaneously for a given blend.

ΔT. The uncertainty in B is ±100 K, in T_0 is ±15 K, in both β and a_{lib} is ±0.1.

Segmental Correlation Times. The segmental correlation times $\tau_{seg,c}$ of the PVE homopolymer and the PVE component in the blends were calculated from the fit parameters in Table 3 and are presented in Figure 12 as symbols. $\tau_{seg,c}$ of the PVE homopolymer agrees well with the NMR work in the literature[3] after accounting for the difference in glass transition temperatures. The dynamics of the PVE component speed up after mixing with the low-T_g component, dPB.

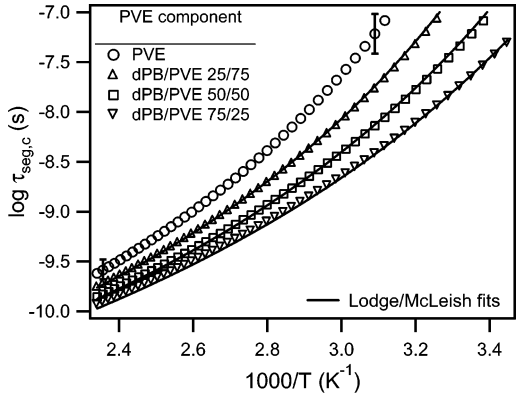

Figure 12. Segmental correlation times (calculated from the fit parameters in Table 3 and shown as symbols) for PVE in the homopolymer and dPB/PVE blends. Representative error bars are shown and reflect the uncertainty associated with the fitting procedure. The solid lines are fits to the Lodge/McLeish model with $\phi_{self}(PVE) = 0.61$.

Comparison to the Lodge/McLeish Model. The Lodge/McLeish model can satisfactorily fit the segmental correlation times of the PVE component in dPB/PVE blends with $\phi_{self}(PVE) = 0.61 \pm 0.06$. The fits are shown in Figure 12 as solid lines. As was the case for the PB component, the fit parameter $\phi_{self}(PVE)$ differs significantly from the model prediction ($\phi_{self} = 0.25$). Possible reasons for this were discussed in section IIIA. With regard to the possibility of "weak coupling" between the segmental dynamics of PB and PVE, it is not clear how this should affect the ϕ_{self} value of the high-T_g component. As discussed above, in PEO/PMMA and PVME/PS blends, the low-T_g components also have unexpected high ϕ_{self} values characterizing their segmental dynamics.[12,25] No measurement of the segmental dynamics has been reported for the PMMA component in PEO/PMMA blends. For the PVME/PS blends, dielectric relaxation data have been reported for the PS component in a limited composition range (80−96% of PS);[9] in this range, the ϕ_{self} value of PS component is close to zero. In this respect the segmental dynamics of the high-T_g component in PS/PVME blends seems quite different than the results reported here for the high-T_g component (PVE) in PB/PVE blends.

Comparison of Segmental and Terminal Dynamics. The segmental dynamics $\tau_{seg,c}$ and the terminal dynamics ζ/T of the PVE component are compared in Figure 13. The left and right axes are offset in order to overlap the PVE homopolymer results. For the PVE homopolymer, the terminal dynamics have the same temperature dependence as the segmental dynamics, as expected. From the figure, it also appears that the terminal and segmental dynamics of the PVE component in dPB/PVE blends have almost the same temperature and composition dependences. This impression is misleading because of the different T_g values in our work and in ref 16. Our work carefully matched the molecular weights in ref 16, but the PVE T_gs differ by 11 K due to different microstructures. To account for this difference, ϕ_{self} values for the segmental and terminal relaxation were compared as suggested in section IIIA. The segmental dynamics of PVE have a

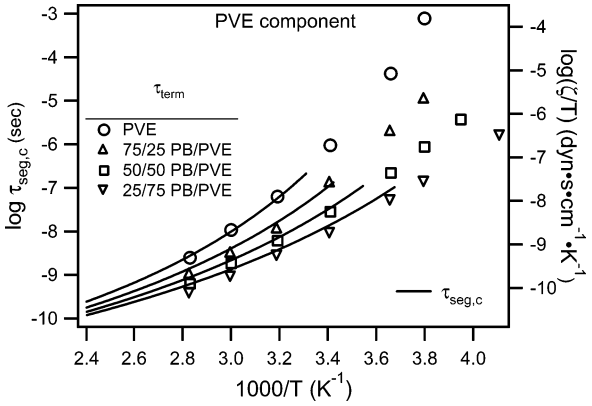

Figure 13. Comparison of the segmental and terminal dynamics for PVE in the homopolymer and dPB/PVE blends. The solid lines are the segmental correlation times calculated from the fit parameters in Table 3. The symbols are the terminal dynamics from ref 16, shifted to lower temperature by 11 K to account for the difference in homopolymer T_g. Note that the segmental correlation times are read on the left axis while the terminal dynamics are read on the right axis.

ϕ_{self} value of 0.61 ± 0.09, while the terminal dynamics have a ϕ_{self} value of 0.43 ± 0.05. Thus, the terminal dynamics of PVE in PB/PVE have a somewhat stronger composition dependence than the segmental dynamics, though not such a dramatic difference as in the case of PB.

C. Comparison of PB/PVE and PI/PVE Blends. For both components in PB/PVE blends, the terminal dynamics exhibit stronger composition dependence than the segmental dynamics. This is in contrast to the results reported for PI/PVE blends, in which the segmental and terminal dynamics exhibit essentially equivalent dependences on the temperature and composition for both components.[1,23] The difference between the two systems is surprising. We had anticipated that the PB/PVE system would behave very similarly to the PI/PVE system, given that PI and PB have similar structures and T_g values, and that χ for both blend systems is quite close to zero. As discussed above, we speculate that the subtle chemical difference between PI and PB (a methyl group) plays a critical role because its absence allows segmental relaxation of PB in the PB/PVE blends under conditions where segmental relaxation of PI in PI/PVE blends would not be possible. However, longer length scale relaxation of the PB chains in the blends cannot occur via this "weak coupling" mechanism and thus the terminal relaxation is more strongly influenced by the PVE component (and quite closely follows the Lodge/McLeish model prediction).

It is interesting to compare the fitted ϕ_{self} values for PVE components in PB/PVE and PI/PVE[23] blends. An assumption of the Lodge/McLeish approach is that ϕ_{self} value for a given polymer should be transferable from one blend to another. To allow a fair comparison, here we determined the ϕ_{self} values by fitting the segmental and terminal dynamics of the PVE component in the same dynamic window for both PI/PVE and PB/PVE blends. For the segmental dynamics, ϕ_{self}(PVE) in the PB/PVE blends (0.61 ± 0.09) is much different than in the PI/PVE blends (0.28 ± 0.05). This might be due to the "weak coupling" of the segmental dynamics. If this conjecture is correct, we would expect similar ϕ_{self} values for the terminal dynamics of PVE in both blend systems due to strong coupling at the terminal level. For the terminal dynamics, ϕ_{self}(PVE) in the PB/PVE blends (0.43 ± 0.05) is about the same as in the PI/PVE blends (0.4 ± 0.1). Although the molecular weights of the PVE are different in the two systems, we do not anticipate that this difference is important since a previous study[23] has found that the monomeric friction factor ζ (terminal dynamics) of PVE in PI/PVE blends is independent of molecular weight.

IV. Conclusions

We have investigated the segmental dynamics of PB in blends with dPVE and of PVE in blends with dPB. The experiments were specifically designed to match the samples used by Yang et al.[16] and thus unambiguously explore the relationship between the component segmental and terminal dynamics in PB/PVE blends. ^{13}C NMR relaxation measurements were performed on the protio components in each series of blends over a wide range of temperature and composition at two magnetic fields. The segmental correlation times were extracted by fitting the NMR data, discussed in the framework of the Lodge/McLeish model, and compared to the terminal dynamics reported in ref 16. In PB/PVE blends, the segmental correlation times for both components were well described by the Lodge/McLeish model as expected, but with the fit parameters ϕ_{self} larger than the model prediction.

For both components in the PB/PVE blends, the terminal dynamics exhibit stronger composition dependence than the segmental dynamics of that component. This is a different result than that reported for PI/PVE blends, in which the segmental and terminal dynamics exhibit essentially equivalent dependences on the temperature and composition for both components. The difference in dynamic behaviors between PB/PVE and PI/PVE blends and the unusually large ϕ_{self} values in PB/PVE blends can be reasonably reconciled by "weak coupling" in segmental dynamics due to the absence of side groups for PB. Given these observations, it seems possibly that terminal dynamics will be more reliably described by models of the Lodge/McLeish type (i.e., transferable ϕ_{self} values) than will be the segmental dynamics.

Acknowledgment. This work is supported by the National Science Foundation (DMR-0355470) and in part by a fellowship from the Merck Research Laboratories (Y.H.). We thank Prof. Paul Nealey for the use of the DSC. Some measurements were performed at the Instrument Center of the Department of Chemistry, University of Wisconsin—Madison, supported by NSF CHE-9629688.

Supporting Information Available: A table summarizing the experimental ^{13}C T_1 and NOE data for the trans units of the PB component in PB/dPVE blends at 125.8 and 25.1 MHz. This material is available free of charge via the Internet at http://pubs.acs.org.

References and Notes

(1) Chung, G. C.; Kornfield, J. A.; Smith, S. D. *Macromolecules* **1994**, *27*, 5729−5741.

(2) Alegria, A.; Colmenero, J.; Ngai, K. L.; Roland, C. M. *Macromolecules* **1994**, *27*, 4486−4492.

(3) Min, B. C.; Qiu, X. H.; Ediger, M. D.; Pitsikalis, M.; Hadjichristidis, N. *Macromolecules* **2001**, *34*, 4466−4475.

(4) Zawada, J. A.; Fuller, G. G.; Colby, R. H.; Fetters, L. J.; Roovers, J. *Macromolecules* **1994**, *27*, 6861−6870.

(5) Doxastakis, M.; Kitsiou, M.; Fytas, G.; Theodorou, D. N.; Hadjichristidis, N.; Meier, G.; Frick, B. *J. Chem. Phys.* **2000**, *112*, 8687−8694.
(6) Adams, S.; Adolf, D. B. *Macromolecules* **1999**, *32*, 3136−3145.
(7) Zetsche, A.; Fischer, E. W. *Acta Polym.* **1994**, *45*, 168−175.
(8) Cendoya, I.; Alegria, A.; Alberdi, J. M.; Colmenero, J.; Grimm, H.; Richter, D.; Frick, B. *Macromolecules* **1999**, *32*, 4065−4078.
(9) Urakawa, O.; Sugihara, T.; Adachi, K. *Polym. Appl. (Jpn.)* **2002**, *51*, 10−17.
(10) Colby, R. H. *Polymer* **1989**, *30*, 1275−1278.
(11) Lartigue, C.; Guillermo, A.; CohenAddad, J. P. *J. Polym. Sci., Polym. Phys.* **1997**, *35*, 1095−1105.
(12) Lutz, T. R.; He, Y. Y.; Ediger, M. D.; Cao, H. H.; Lin, G. X.; Jones, A. A. *Macromolecules* **2003**, *36*, 1724−1730.
(13) Chin, Y. H.; Inglefield, P. T.; Jones, A. A. *Macromolecules* **1993**, *26*, 5372−5378.
(14) Kim, E.; Kramer, E. J.; Osby, J. O. *Macromolecules* **1995**, *28*, 1979−1989.
(15) Urakawa, O.; Fuse, Y.; Hori, H.; Tran-Cong, Q.; Yano, O. *Polymer* **2001**, *42*, 765−773.
(16) Yang, X. P.; Halasa, A.; Hsu, W. L.; Wang, S. Q. *Macromolecules* **2001**, *34*, 8532−8540.
(17) Katana, G.; Fischer, E. W.; Hack, T.; Abetz, V.; Kremer, F. *Macromolecules* **1995**, *28*, 2714−2722.
(18) Chapman, B. R.; Hamersky, M. W.; Milhaupt, J. M.; Kostelecky, C.; Lodge, T. P.; von Meerwall, E. D.; Smith, S. D. *Macromolecules* **1998**, *31*, 4562−4573.
(19) He, Y. Y.; Lutz, T. R.; Ediger, M. D. *Macromolecules* **2003**, *36*, 8040−8048.
(20) Haley, J. C.; Lodge, T. P. *J. Rheol.* **2004**, *48*, 463−486.
(21) Savin, D. A.; Larson, A. M.; Lodge, T. P. *J. Polym. Sci., Polym. Phys.* **2004**, *42*, 1155−1163.
(22) Pathak, J. A.; Kumar, S. K.; Colby, R. H. *Macromolecules* **2004**, *37*, 6994−7000.
(23) Haley, J. C.; Lodge, T. P.; He, Y. Y.; Ediger, M. D.; von Meerwall, E. D.; Mijovic, J. *Macromolecules* **2003**, *36*, 6142−6151.
(24) He, Y. Y.; Lutz, T. R.; Ediger, M. D.; Lodge, T. P. *Macromolecules* **2003**, *36*, 9170−9175.
(25) He, Y. Y.; Lutz, T. R.; Ediger, M. D. *J. Chem. Phys.* **2003**, *119*, 9956−9965.
(26) Lodge, T. P.; McLeish, T. C. B. *Macromolecules* **2000**, *33*, 5278−5284.
(27) Adachi, K.; Kotaka, T. *Macromolecules* **1984**, *17*, 120−122.
(28) Roland, C. M.; Ngai, K. L.; Santangelo, P. G.; Qiu, X. H.; Ediger, M. D.; Plazek, D. J. *Macromolecules* **2001**, *34*, 6159−6160.
(29) He, Y. Y.; Lutz, T. R.; Ediger, M. D.; Ayyagari, C.; Bedrov, D.; Smith, G. D. *Macromolecules* **2004**, *37*, 5032−5039.
(30) Balsara, N. P. *Physical Properties of Polymers Handbook;* AIP Press: Woodbury, NY, 1996; Chapter 19.
(31) Kaplan, M. L.; Bovey, F. A.; Cheng, H. N. *Anal. Chem.* **1975**, *47*, 1703−1705.
(32) Wang, H. T.; Bethea, T. W.; Harwood, H. J. *Macromolecules* **1993**, *26*, 715−720.
(33) Lyerla, J. R.; Levy, G. C. *Top. Carbon-13 NMR Spectrosc.* **1974**, *1*, 79.
(34) Heatley, F. *Prog. Nucl. Magn. Reson. Spectrosc.* **1979**, *13*, 47−85.
(35) Heatley, F. *Annu. Rep. NMR Spectrosc.* **1986**, *17*, 179−230.
(36) Gisser, D. J.; Glowinkowski, S.; Ediger, M. D. *Macromolecules* **1991**, *24*, 4270−4277.
(37) Bandis, A.; Wen, W. Y.; Jones, E. B.; Kaskan, P.; Zhu, Y.; Jones, A. A.; Inglefield, P. T.; Bendler, J. T. *J. Polym. Sci., Polym. Phys.* **1994**, *32*, 1707−1717.
(38) Moe, N. E.; Qiu, X. H.; Ediger, M. D. *Macromolecules* **2000**, *33*, 2145−2152.
(39) Qiu, X. H.; Moe, N. E.; Ediger, M. D.; Fetters, L. J. *J. Chem. Phys.* **2000**, *113*, 2918−2926.
(40) Tammann, G.; Hesse, W. *Z. Anorg. Allg. Chem.* **1926**, *156*, 245.
(41) Williams, M. L.; Landel, R. F.; Ferry, J. D. *J. Am. Chem. Soc.* **1955**, *77*, 3701−3707.
(42) Laupretre, F.; Monnerie, L.; Roovers, J. *PMSE Prepr.* **2000**, *82*, 154.
(43) Hofmann, A.; Alegria, A.; Colmenero, J.; Willner, L.; Buscaglia, E.; Hadjichristidis, N. *Macromolecules* **1996**, *29*, 129−134.
(44) Arbe, A.; Richter, D.; Colmenero, J.; Farago, B. *Phys. Rev. E* **1996**, *54*, 3853−3869.
(45) Deegan, R. D.; Nagel, S. R. *Phys. Rev. B* **1995**, *52*, 5653−5656.
(46) Smith, G. D.; Borodin, O.; Bedrov, D.; Paul, W.; Qiu, X. H.; Ediger, M. D. *Macromolecules* **2001**, *34*, 5192−5199.
(47) Zorn, R.; Mopsik, F. I.; McKenna, G. B.; Willner, L.; Richter, D. *J. Chem. Phys.* **1997**, *107*, 3645−3655.
(48) The simulations were carried out on PB chains with a molecular weight of 1600 g/mol. NMR relaxation measurements were performed on a PB sample with the same molecular weight and microstructure as in the simulations (ref 46). There is a 11 K temperature shift between the NMR data of the two samples (in ref 46 and here).
(49) Roland, C. M.; Ngai, K. L. *J. Rheol.* **1992**, *36*, 1691−1706.
(50) In Figure 8, the largest ratio is 1 decade (for PB in PB/dPVE 25/75 blend at the lowest temperature end). In the same plot for *trans*-PB units, the largest ratio is 0.8 decade.
(51) We used $n = 1.5$ in fitting the data since T_1 values of the methylene and methine backbone carbons were averaged.

MA048419N